IFNL3 (IL28B) favorable genotype escapes hepatitis C virus-induced microRNAs and mRNA decay

Published in final edited form as:
Nat Immunol. 2014 January ; 15(1): 72–79. doi:10.1038/ni.2758.

IFNL3 (*IL28B*) favorable genotype escapes hepatitis C virus-induced microRNAs and mRNA decay

Adelle P. McFarland[1], **Stacy M. Horner**[1,7], **Abigail Jarret**[1], **Rochelle C. Joslyn**[1], **Eckart Bindewald**[2], **Bruce A. Shapiro**[3], **Don A. Delker**[4], **Curt Hagedorn**[4], **Mary Carrington**[5,6], **Michael Gale Jr.**[1], and **Ram Savan**[1]

[1]Department of Immunology, University of Washington, Seattle, Washington, USA.

[2]Basic Science Program, SAIC-Frederick, Frederick National Laboratory for Cancer Research, Frederick, Maryland, USA.

[3]Center for Cancer Research Nanobiology Program, Frederick National Laboratory for Cancer Research, Frederick, Maryland, USA.

[4]Divison of Gastroenterology, Hepatology and Nutrition, School of Medicine, University of Utah, Salt Lake City, Utah, USA.

[5]Cancer and Inflammation Program, Laboratory of Experimental Immunology, SAIC-Frederick, Inc., Frederick National Laboratory for Cancer Research, Frederick, Maryland, USA.

[6]Ragon Institute of Massachusetts General Hospital, Massachusetts Institute of Technology and Harvard University, Boston, Massachusetts, USA.

Abstract

The *IFNL3* (*IL28B*) gene has received immense attention in the hepatitis C virus (HCV) field as multiple independent genome-wide association studies identified a strong association between polymorphisms near the *IFNL3* gene and HCV clearance. However, the mechanism underlying this association has remained elusive. In this study, we report the identification of a functional polymorphism (rs4803217) located in the 3′ untranslated region (3′ UTR) of the *IFNL3* mRNA that dictates transcript stability. This polymorphism influences AU-rich element-mediated decay as well as the binding of HCV-induced microRNAs during infection. Together, these pathways mediate robust repression of the unfavorable *IFNL3* genotype. These data reveal a novel mechanism by which HCV attenuates the antiviral response and uncover new potential therapeutic targets for HCV treatment.

Correspondence and requests for materials should be addressed to: R.S. (savanram@u.washington.edu).
[7]Present address: Department of Molecular Genetics and Microbiology, Center for Virology, Duke University Medical Center, Durham, North Carolina, USA.

AUTHOR CONTRIBUTIONS

A.P.M. and R.S. designed the study and wrote the manuscript. R.S. directed the study. A.P.M. analyzed the data. A.P.M., A.J., R.S. and R.C.J. performed ARE and miRNA experiments. S.M.H. performed infections and flow cytometry preparations. E.B. and B.A.S. generated base pairing probabilities. C.H. and D.A.D. contributed clinical samples. M.C. and M.G. provided intellectual input.

AUTHOR INFORMATION

The authors declare no competing financial interests.

Hepatitis C virus (HCV) infects over 150 million people worldwide. Treatment for chronic HCV infection is based on interferon (IFN) combination therapy with ribavirin. A newly approved triple combination treatment, which includes direct-acting antiviral (DAA) agents, has improved viral cure rates to greater than 60%[1]. However, emergence of therapy-resistant HCV variants in patients treated with DAAs has become an important concern[1,2]. Genome-wide association studies (GWAS) have identified three single nucleotide polymorphisms (SNPs) near the *IFNL3* (*IL28B*) gene that strongly associate with HCV patient response to therapy[3–6] and natural clearance of infection[6,7]. However, the functional polymorphism mediating these associations is still unknown.

IFNL3 is a member of the interferon-λ (IFNL) cytokine family, which is comprised of IFNL1 (IL-29), IFNL2 (IL-28A) and IFNL3, all of which are encoded by genes clustered on human chromosome 19[8,9]. IFNLs are induced in both hematopoietic and nonhematopoietic cells by various human viruses[10]. Unlike IFN-α/β, IFNL signaling exhibits cellular specificity as the IFNL receptor is narrowly distributed on epithelial cells, melanocytes and hepatocytes, suggesting that IFNLs represent a family of cytokines that evolved to specifically protect epithelia from viral invasion[11]. IFNLs are potent antiviral cytokines that have the ability to inhibit HCV replication, and when paired with DAAs have shown comparable antiviral activity against HCV to IFN-α[12,13]. IFNL and IFN-α induce a similar repertoire of IFN-stimulated genes (ISG) in human hepatocytes, although treatment with IFNL induces a steady increase in expression instead of the rapid peak and decline seen with IFN-α[12,14]. Several confounding studies have shown that the *IFNL3* unfavorable genotype associates with higher pre-therapy ISG levels during HCV infection[15,16]. However, correlations between ISG levels and *IFNL3* genotype have been shown to differ by cell type[16], and when treatment response (non-responders versus responders) is stratified by *IFNL3* genotype, there is no difference in total mean baseline ISG expression[17]. This suggests that *IFNL3* genotype and pre-therapy ISG levels are independent predictors of IFN responsiveness in chronic HCV patients[17].

While five studies have found a correlation between *IFNL3* genotype and IFNL3 expression[3,4,18–20], where higher IFNL3 levels associate with clearance, three studies found no association[5,15,21]. One study which demonstrated an association in normal liver also found that individuals with the favorable *IFNL3* genotype expressed the highest levels of ISGs[19]. As discussed, this is opposite to what has been found in baseline gene expression analyses of chronic HCV patients, suggesting that chronic infection dysregulates the immune response making correlations between *IFNL3* genotype and gene expression less straightforward. Furthermore, cytokine mRNAs are extremely labile in nature, making them very difficult to measure in biological samples. As there are substantial data supporting a correlation between *IFNL3* genotype and IFNL3 expression, we set out to determine whether there is a functional variant that mediates expression differences of this cytokine.

Four candidate causal SNPs have been identified that are in linkage disequilibrium with the GWAS SNPs[22–24]. None of these candidate SNPs, which are located in the *IFNL3* promoter, intron, coding region or 3′ untranslated region (UTR), have been previously shown to functionally affect *IFNL3* expression. As cytokine gene expression is under tight post-transcriptional control[25], we hypothesized that variation in the *IFNL3* 3′ UTR (SNP

rs4803217) might alter mRNA turnover and protein expression by interfering with regulatory elements. The frequency of the rs4803217 T variant (unfavorable genotype) is more common amongst African populations (T=55%, G=45%) and least common in Asians (T=7%. G=93%) (www.1000genomes.org). A similar frequency is seen for the GWAS tag SNP rs12979860, which is in linkage disequilibrium with the 3′ UTR SNP. The differences in frequency between populations has been proposed as the reason why individuals of African descent are less likely to clear HCV than Asians, as the unfavorable genotype is more frequent in those patients[7]. In this study, we show that SNP rs4803217 is responsible for robust expression differences between clearance (G/G) and non-clearance (T/T) *IFNL3* genotypes thus identifying rs4803217 as a critical functional SNP that directs HCV infection outcome through the control of *IFNL3* mRNA stability. Our data reveal HCV induction of two microRNAs, miR-208b and miR-499a-5p, which target the polymorphic region of the *IFNL3* 3′ UTR, as a novel strategy of immune evasion by HCV and propose these microRNAs as therapeutic targets for restoring the host antiviral response.

RESULTS

Influence of 3′ UTR SNP rs4803217 on *IFNL3* mRNA

We evaluated the influence of the 3′ UTR rs4803217 SNP on the post-transcriptional regulation and stability of the *IFNL3* mRNA. Full-length *IFNL3* 3′ UTRs containing either a T (*IFNL3*-T) or G (*IFNL3*-G) at position 53 in the 3′ UTR were cloned downstream of the luciferase gene in a pGL3 reporter construct (Fig. 1a **and** Supplementary Fig. 1a, b) and luciferase activity was measured in transfected human hepatoma (HepG2 and Huh7) cells. The *IFNL3*-T 3′ UTR conferred 30–40% lower luciferase activity compared to the *IFNL3*-G 3′ UTR (Fig. 1b). We next assessed the effect of rs4803217 on mRNA stability. Analysis of firefly luciferase mRNA levels remaining in HepG2 cells post-Actinomycin D treatment revealed that luciferase mRNA bearing the *IFNL3*-T 3′ UTR decayed twice as fast compared to the *IFNL3*-G 3′ UTR, demonstrating that this single nucleotide change affected the general stability of the mRNA transcript (Fig. 1c). Taken together, these data show that rs4803217 strongly influences the stability and expression of *IFNL3*.

Like many cytokines, the *IFNL3* 3′ UTR contains *cis*-acting repetitive adenosine-uridine stretches or AU-rich elements (ARE) (positions 33–37, 58–62 and 79–83; Fig. 1d and Supplementary Fig. 1a). AREs are perhaps the best-known determinants of mRNA stability as degradative RNA-binding proteins can bind to AREs leading to ARE-mediated decay (AMD) of the transcript[26]. *IFNL3* can be categorized as a class I ARE-containing mRNA, as it has 3 copies of the pentameric motif AUUUA. We generated *IFNL3* 3′ UTR luciferase reporter constructs with disrupted ARE motifs (Fig. 1d; ΔARE, AUUUA→AUCUA) and measured luciferase expression in transfected HepG2 cells. Both the *IFNL3*-T ΔARE and *IFNL3*-G ΔARE 3′ UTRs were completely protected from repression, showing equivalent rescue over the *IFNL3*-T and *IFNL3*-G 3′ UTRs (Fig. 1e). These data demonstrate that the AREs in the *IFNL3* 3′ UTR are functional and facilitate AMD of this cytokine.

The expression differences between *IFNL3*-T and G were not maintained in the absence of AMD, suggesting that AMD may have a stronger impact on *IFNL3*-T stability. To explore this further, we generated luciferase reporter constructs with individual ARE sites (1–3)

disrupted in both the *IFNL3*-T and *IFNL3*-G 3′ UTRs. We observed that the differential regulation of *IFNL3*-T versus G was only maintained in the presence of both ARE 1 and ARE 2 and did not require activity at ARE 3 (Fig. 1f). However, when ARE 1 or ARE 2 were disrupted individually, the difference in degradation between the *IFNL3*-T and *IFNL3*-G 3′ UTRs was not significant. This suggested that ARE 3 participated in equal degradation of both variants, whereas the combined activity of AREs 1 and 2 facilitated differential AMD. It is possible that the location of rs4803217 between ARE 1 and ARE 2 alters the local secondary structure of the mRNA thereby disrupting the ability of ARE-binding proteins to effectively degrade the *IFNL3*-T mRNA. Comparisons between predicted base pair probabilities of *IFNL3*-T versus *IFNL3*-G 3′ UTRs showed that the only sites with significant differences between the 3′ UTR variants were ARE 1, ARE 2 and the rs4803217 SNP (Supplementary Fig. 1c). Structural changes in motif-defining sequences, such as AREs, within the 3′ UTR can have functional consequences by influencing accessibility to *trans*-acting RNA decay factors[27].

The IFNL2 and IFNL3 cytokines have 98% amino acid sequence similarity[8,9] and 95% 3′ UTR sequence identity (Supplementary Fig. 1a). In contrast, the 3′ UTRs of *IFNL3* and *IFNL1* have a low sequence identity (47%) but do share conservation within the AREs (Supplementary Fig. 2a). The *IFNL3* 3′ UTR T variant of rs4803217 is the ancestral allele and only in humans has a G variant emerged (Supplementary Fig. 2b). Interestingly, there are no known *IFNL2* variants that associate with HCV clearance. In contrast to type I and type II IFNs, the IFNL members have been strongly affected by positive selection[28]. This previous analysis revealed that five SNPs near or in the *IFNL3* gene, including rs4803217, have rapidly increased in frequency. However, position 53 (which aligns with rs4803217 in the *IFNL3* 3′ UTR) is fixed in the 3′ UTR of *IFNL2* with a T nucleotide. To understand why the polymorphism at this site was evolutionary selected for in *IFNL3* and not *IFNL2*, we cloned into luciferase reporter constructs the full-length *IFNL2* 3′ UTR as well as one in which the native T nucleotide at position 53 was replaced with a G (*IFNL2* T→G) (Supplementary Fig. 2c). When expressed in HepG2 cells, the luciferase activity of the *IFNL2* wild type T 3′ UTR construct was significantly higher (+15%) than *IFNL3*-T (Fig. 1g). The *IFNL2* T→G 3′ UTR resulted in only a small increase in luciferase activity compared to the expression of the wild type 3′ UTR. We also investigated whether a ΔARE *IFNL2* 3′ UTR would rescue the expression of the luciferase reporter and found that, like the *IFNL3* ΔARE 3′ UTRs, it was completely protected from repression (Supplementary Fig. 2d). Overall these data indicate that like *IFNL3*, *IFNL2* mRNA is subjected to post-transcriptional regulation by AMD but is not degraded to the same extent as *IFNL3*-T.

microRNA regulation of *IFNL2* and *IFNL3*

Since a 3′ UTR variant of *HLA-C* is known to strongly associate with control of HIV infection and drives high expression of *HLA-C* by escaping regulation by miR-148[29], we reasoned such a mechanism could operate on *IFNL3*. miRNAs are a class of small (~22 nucleotides) regulatory RNA molecules whose main function is to decrease protein-coding mRNA levels by directly pairing with the target 3′ UTR mRNA[30]. Recent work has demonstrated that miRNAs can cooperate with ARE-binding proteins to destabilize cytokines[31]. We investigated whether the rs4803217 3′ UTR SNP, in addition to mediating

differential AMD, could influence recruitment of miRNAs to the *IFNL3* 3′ UTR. We examined the 3′ UTR sequence around rs4803217 for predicted miRNA binding sites and identified potential binding sites for hsa-miR-208b and hsa-miR-499a-5p, two miRNAs with identical seed regions in the *IFNL3*-T and *IFNL2* 3′ UTRs (Fig. 2a **and** Supplementary Fig. 1a). The rs4803217 T→G SNP is in the miRNA seed region and is therefore predicted to prevent the binding of these miRNAs to the *IFNL3*-G 3′ UTR.

The *MIR208B* and *MIR499A* genes are encoded within the introns of two myosin genes, myosin heavy chain 7 (*MYH7*) and myosin heavy chain 7B (*MYH7B*), respectively (Fig. 2b). They are part of a group of miRNAs termed ‘myomiRs’ due to their location and coexpression with their corresponding myosin genes[32]. A key feature of these myomiRs is their restricted expression to cardiac and slow skeletal muscle, as *MYH7* and *MYH7B* encode the major contractile proteins of muscle. In this setting, miR-208b and miR-499a-5p control myosin expression and skeletal myofiber phenotypes by targeting transcriptional repressors of myofiber genes[32]. As these miRNAs are not normally expressed in the liver and were not detectable constitutively in HepG2 or Huh7 cells, we tested if HCV infection could induce their expression. We found that HCV infection strongly induced expression of the myosin genes and their myomiRs (Fig. 2c, d **and** Supplementary Fig. 3a). Another myomiR family member encoded in the myosin gene *MYH6*, miR-208a, has a seed sequence identical to that of miR-208b and miR-499a-5p and was predicted to target the *IFNL3*-T 3′ UTR, but we could not detect its induction by HCV infection. Therefore, in this study, we set out to characterize the effects of the HCV-inducible myomiRs, miR-208b and miR-499a-5p, on the 3′ UTRs of *IFNL2* and *IFNL3*.

We co-transfected HepG2 cells with miR-208b, miR-499a-5p or negative control mimics and luciferase reporter constructs containing the *IFNL3*-T, *IFNL3*-G or *IFNL2* 3′ UTR. Both miR-208b and miR-499a-5p significantly reduced the luciferase activity of the *IFNL3*-T 3′ UTR but not the *IFNL3*-G 3′ UTR compared to the negative control (Fig. 2e). To test whether ARE-binding proteins are involved in the recruitment of the miRNA-induced silencing complex (miRISC) to the *IFNL3* 3′ UTR, we co-transfected the myomiR mimics with the *IFNL3* ΔARE luciferase reporter constructs. Similar to results obtained with the *IFNL3*-T and *IFNL3*-G 3′ UTRs, the myomiRs were able to repress the *IFNL3*-T ΔARE 3′ UTR but had no significant effect on the *IFNL3*-G ΔARE 3′ UTR (Supplementary Fig. 3b). Therefore, ARE-binding proteins are not physically required for miRISC recruitment to the *IFNL3*-T 3′ UTR. Luciferase activity of the *IFNL2* 3′ UTR was also significantly reduced by the myomiR mimics but was more resilient against low concentrations of the mimics compared to the *IFNL3* 3′ UTR (Fig. 2e and Supplementary Fig. 3c). Overall these results demonstrate that miR-208b and miR-499a-5p can directly target and mediate degradation of the *IFNL3*-T 3′ UTR and that the T→G rs4803217 SNP confers protection against repression by these myomiRs.

We found that the *IFNL3* genotype of our HepG2 cell line is T/T at position rs4803217, so we used these cells to study possible myomiR regulation of endogenous *IFNL2* and *IFNL3* transcripts. We treated HepG2 cells with the Toll-like receptor 3 (TLR3) ligand Poly(I:C) and observed peak *IFNL* mRNA expression around 12 h post-stimulation (Supplementary Fig. 3d). When HepG2 cells were transfected with miR-208b, miR-499a-5p or negative

control mimics and then stimulated with Poly(I:C), we observed that both myomiRs significantly repressed expression of *IFNL2* and *IFNL3* mRNA (Fig. 2f). To assess whether this repression was a result of mRNA destabilization, we analyzed the stability of the mRNA in the presence of the myomiR mimics following Actinomycin D treatment. To induce *IFNL*, we stimulated HepG2 cells with the HCV 3′ poly U/UC tract, a pathogen-associated molecular pattern (PAMP) of HCV encoded within the 3′ UTR that has potent immunostimulatory effects on hepatocytes, such as inducing type I IFN[33]. We found that the HCV PAMP strongly induced expression of both *IFNL2* and *IFNL3* in HepG2 cells (Supplementary Fig. 3e). miR-208b, miR-499a-5p or negative control mimics as well as HCV PAMP were transfected into HepG2 cells and 16 h post-stimulation new transcription was arrested with Actinomycin D. We observed that miR-208b and miR-499a-5p both reduced the *IFNL2* and *IFNL3* mRNA half-lives to nearly half that observed with negative control mimics (Fig. 2g).

To support direct miRNA targeting of endogenous *IFNL* transcripts, we measured the association of *IFNL2* and *IFNL3* mRNA with the miRISC complex. HepG2 cells were co-transfected with either negative control mimics or a cocktail of miR-208b and miR-499a-5p mimics along with the HCV PAMP for 16 h. We then immunoprecipitated Ago2, one of the major miRISC proteins involved in mRNA cleavage and found significant levels of both *IFNL2* and *IFNL3* mRNA within the Ago2 IP RNA of negative control mimic-treated cells, demonstrating recruitment of miRISC by some endogenous miRNA(s) (Supplementary Fig. 3f). However, the amount of *IFNL2* and *IFNL3* mRNA within the Ago2 IP RNA of cells treated with the myomiR mimics was significantly increased over the negative control mimic-treated cells. We also amplified both miR-208b and miR-499a-5p from the Ago2-associated RNA in the cells transfected with mimics (data not shown). Collectively, these data confirm that miR-208b and miR-499a-5p can directly target and destabilize endogenous *IFNL2* and *IFNL3* transcripts.

HCV-induced myomiRs repress *IFNL3*-T transcripts

To investigate the effect of endogenous HCV-induced myomiRs on the *IFNL3* 3′ UTR variants, we developed reporter constructs containing either the mCherry gene or eGFP with the *IFNL3*-T 3′ UTR or *IFNL3*-G 3′ UTR cloned downstream, respectively (Supplementary Fig. 4a). These reporter constructs allowed for simultaneous expression of the *IFNL3* 3′ UTR variants within the same cells (Supplementary Fig. 4b). Flow cytometric analysis of Huh7 cells co-transfected with these constructs showed the differential expression of *IFNL3*-T versus *IFNL3*-G 3′ UTRs (Fig. 3a) as we had seen previously by luciferase assay (Fig. 1b). To assess whether the HCV-induced myomiRs differentially repressed the *IFNL3* 3′ UTR variants within the same cells, we used this mCherry/eGFP co-expression system along with specific locked nucleic acid (LNA) inhibitors against the induced myomiRs. The LNA inhibitors were designed to inhibit miR-208b and miR-499a-5p with high specificity, and efficiency was demonstrated in HepG2 cells stably overexpressing miR-208b and miR-499a-5p (Fig. 3b). To test the effect of the inhibitors on HCV-induced myomiRs, Huh7 cells were infected with HCV and then co-transfected with the mCherry/eGFP *IFNL3* 3′ UTR reporter constructs and LNA myomiR inhibitors or controls. Mean fluorescent intensities were also compared to uninfected cells with the fluorescent reporters in the

presence or absence of myomiR mimics. Cells infected with HCV suppressed the *IFNL3*-T but not the *IFNL3*-G 3′ UTR reporter (Fig. 3c). The level of repression by the HCV-induced myomiRs was similar to that observed with the mimics. Importantly, inhibition of miR-208b and miR-499a-5p in infected cells resulted in a significant increase in *IFNL3*-T but not *IFNL3*-G expression. Therefore, HCV infection accelerated degradation of mRNA bearing the *IFNL3*-T 3′ UTR but not *IFNL3*-G via the induction of myomiRs.

We next determined the effect of myomiR inhibition on endogenous *IFNL3* transcripts during infection. Huh7 cells are weak producers of IFNs due to a disruption in RIG-I helicase signaling by HCV[34,35]. However, *IFNL2* and *IFNL3* mRNA was detectable in Huh7 cells at 72 h post-infection with a high multiplicity of infection (MOI), so we used these conditions to study the regulation of *IFNL* mRNA by the myomiRs during infection (Fig. 3d–f). Since the genotype of our Huh7 cell line was T/T at rs4803217, we could assess the effect of the inhibitors on virally-induced *IFNL3* in the presence of virally-induced myomiRs. Induction of the myosin genes by HCV was unaffected by the presence of the myomiR inhibitors, while myomiR expression was significantly reduced (Fig. 3d, e). We then assayed for *IFNL* levels and found that the myomiR inhibitors significantly rescued *IFNL2* and *IFNL3* expression over the negative control inhibitor (Fig. 3f). Furthermore, despite the high MOI required for the expression of *IFNL2* and *IFNL3* in this *in vitro* infection system, we were able to observe a significant decrease in viral copy number and titer (Fig. 3g, h). These data demonstrate that HCV-induced miR-208b and miR-499a-5p target the rs4803217 SNP in the *IFNL3* 3′ UTR and that myomiR inhibition can rescue this suppression.

Induction of myosin and myomiRs during HCV infection

To investigate how HCV induces *MYH7* and *MYH7B*, we infected Huh7.5 cells, which are deficient in innate immune signaling by RIG-I, the essential pathogen recognition receptor of HCV infection[36,37], and measured myosin expression. Both *MYH7* and *MYH7B* and their respective myomiRs, miR-208b and miR-499a-5p, were induced to the levels similar to those observed during infection of Huh7 cells (Fig. 4a, Fig. 2c, d and Supplementary Fig. 5a). We also tested for expression of the myosin genes in HepG2 cells stimulated with Poly(I:C) or the HCV PAMP but did not observe any induction (Fig. 4b). Therefore, induction of *MYH7* and *MYH7B* by HCV occurs independently of HCV PAMP-RIG-I signaling, perhaps requiring viral RNA replication or expression of HCV proteins. To test whether the induction of the myosin genes was specific to infection with HCV, we also assessed gene expression in Huh7 cells infected with Sendai virus (SenV) or West Nile virus (WNV). SenV and WNV were comparatively unable to induce *MYH7B* and induced only low levels of *MYH7* expression, despite productive infection and induction of *IFNB* (Fig. 4c and Supplementary Fig. 5b), indicating that the induction of *MYH7* and *MYH7B* may be HCV-specific.

Myosin and myomiRs in chronic hepatitis C patients

To determine if patients with HCV infection exhibit hepatic expression of the myosin and their associated myomiRs, we evaluated liver RNA recovered from chronic hepatitis C patients. Five out of 8 patients tested showed robust expression of *MYH7* that was >200 fold

over the average uninfected control level (Fig. 5a). *MYH7B* was also significantly expressed in these patients over controls (>10 fold in 5/8), albeit at a lower level than *MYH7*, similar to our observation with *in vitro* HCV infection. Also similar to *in vitro* infection, we did not detect elevated *MYH6* expression, which supports a specific pathway of induction for *MYH7* and *MYH7B* (data not shown). Hepatitis C patients also had significantly elevated hepatic levels of miR-208b (Fig. 5a). Although these patients had elevated *MYH7B* expression, we did not detect differences in mature miR-499a-5p. To examine whether this was due to uncoupling of *MYH7B* expression from miR-499a-5p, we also assayed for the presence of primary miR-499a transcripts (pri-miR-499a) and found significantly elevated levels in the hepatitis C patients over controls. Therefore, the inability to detect mature miR-499a-5p does not appear to be the result of an uncoupling from its parental myosin gene and may reflect the limitation of qRT-PCR primers in detecting mature miR-499a-5p isomiRNAs in the liver, which present obstacles for detecting mature miRNA within different tissues[38,39]. However, we did observe a significant correlation between expression of *MYH7* and miR-208b as well as *MYH7B* with pri-miR-499a in the patients examined, demonstrating that *MYH7* mRNA levels are a reliable readout for miR-208b expression (Fig. 5b). Overall, these observations demonstrate that HCV induces hepatic expression of cardiac and skeletal myosin genes and associated myomiRs in infected individuals which supports the proposed mechanism of repression of *IFNL2* and *IFNL3*-T during infection (Supplementary Fig. 6).

DISCUSSION

The work presented here demonstrates a previously undescribed mechanism by which HCV attenuates the hepatic innate immune IFN response. These data suggest that targeted inhibition of miR-208b and miR-499a-5p could rescue IFNL2 and IFNL3 levels to impart control of HCV infection. Inhibition of miR-122, which is required for HCV replication, has recently shown promising results in clinical trials demonstrating the feasibility of anti-miRNA therapy[40]. Therefore, inhibition of HCV-induced myomiRs has the potential to become an important part of treating HCV infection and mitigating progression to cirrhosis and liver cancer. As miR-208b and miR-499a-5p are encoded within cardiac and skeletal muscle-specific myosin heavy chain genes, it is interesting to note that a high prevalence of HCV infection has been reported in patients with hypertrophic cardiomyopathy, dilated cardiomyopathy, and myocarditis[41]. Furthermore, autoantibodies against cardiac myosin, including the myosin heavy chains, are commonly observed in patients with all of these cardiac diseases[42,43], suggesting that aberrant induction of cardiac myosin within the liver by HCV may indirectly contribute to cardiac pathology.

Our comparative analysis of the *IFNL2* and *IFNL3* 3′ UTRs revealed that despite the significant difference in luciferase expression observed between the T and G variants of *IFNL3*, the same base pair change in the *IFNL2* 3′ UTR did not result in an increase of similar magnitude. If the presence of the G variant in the *IFNL3* 3′ UTR is the result of genetic selection for increased IFNL3 levels during HCV infection, these data may explain why no such variant exists for *IFNL2*. Namely, *IFNL2* is expressed at higher levels compared to the *IFNL3*-T variant and a T→G change in *IFNL2* results in only a small increase in expression. Therefore, this change in *IFNL2* may not confer a host advantage during HCV infection. Additionally, IFNL3 has been shown to have higher ISG stimulatory

activity than IFNL2, which may make an *IFNL3* escape variant more evolutionarily advantageous, as it has a greater capacity to establish an antiviral state[13,44].

In this study, we have identified a functional *IFNL3* variant that associates with HCV clearance. Our results reveal that the rs4803217 T→G SNP in the *IFNL3* 3' UTR increases expression of *IFNL3* by escaping both AMD and post-transcriptional regulation by HCV-induced miRNAs. Between these two mechanisms of post-transcriptional regulation, *IFNL3*-T suffers significantly more degradation than *IFNL3*-G. A frameshift variant upstream of *IFNL3* has been described that creates a novel gene, *IFNL4*[45]. Expression of *IFNL4* was associated with HCV persistence and poorer response to IFN plus ribavirin therapy. Therefore, it may be the combined effect of IFNL4 and low expression of IFNL3 that makes this haplotype so unfavorable for HCV infection and treatment outcome. However, previous work has shown that the *IFNL* genes are in low linkage disequilibrium in all populations, suggesting that independent positive selection events are targeting these genes[28]. Our data also show that HCV infection is specifically able to induce miRNAs that interact with rs4803217 and this may explain why the *IFNL3* locus has been found only to associate with HCV and no other viral infection. Additionally, HCV genotypes may vary in their ability to effectively induce the miRNAs which may explain why the *IFNL3* GWAS SNPs do not uniformly associate with response to therapy across infections with all HCV genotypes. Thus, the identification of this causal *IFNL3* 3′ UTR SNP provides a potentially important link between host and HCV genetics.

ONLINE METHODS

Cell lines and culture conditions

HepG2, Huh7 or Huh7.5 cells were grown in DMEM (Sigma) medium with 10% heat-inactivated fetal bovine serum (FBS; Atlanta Biologicals) and 1% penicillin-streptomycin-glutamine (Mediatech) at 37°C in 5% CO_2.

Genotype analysis of rs4803217

The *IFNL3* locus, including the 3′ UTR, was amplified from genomic DNA extracted from HepG2 or Huh7 cells using the following primer pair: forward 5′-gagcaggtggaatcctcttg-3′ and reverse 5′-agcaggcaccttgaaatgtc-3′. The PCR product was then genotyped at rs4803217 according to the ABI TaqMan genotyping assay procedure with the following primer pair and probes: forward primer 5′-gccagtcatgcaacctgagatttta-3′ and reverse primer 5′-aaatacataaatagcgactgggtgaca-3′; probe for *IFNL3*-T 5′-FAM-ttagccacttgtcttaat-NFQMGB-3′ and probe for *IFNL3*-G 5′-VIC-tagccacttggcttaat-NFQMGB-3′.

Secondary structure prediction

Per-residue base pair probabilities of *IFNL3*-T and *IFNL3*-G were computed as a column-wise sum of the predicted base probability matrix using the RNAfold program (Vienna RNA package, version 2.0.0, using option “-p”)[46].

Construction of human *IFNL2* and *IFNL3* 3′ UTR luciferase reporters

Full-length 3′ UTRs (Supplementary Fig. 1a) for human *IFNL2* (containing either a T or G at 3′ UTR position 53) and *IFNL3* (containing either a T or G at SNP rs4803217) were cloned in an *Xba*I site downstream of the luciferase gene in the pGL3 reporter vector (Promega). *IFNL2* and *IFNL3*-T 3′ UTR luciferase constructs containing disrupted AREs were created by introducing a C instead of a T nucleotide (ATTTA→ATCTA) in all three ATTTA motifs (synthesized by Life Technologies). *IFNL3*-T 3′ UTRs with individual ARE sites disrupted were synthesized and subcloned into the pGL3 vector. The following primers: forward 5′-tttatctataaattagccac ttgtcttaatctattgtcacccagtcg-3′ and reverse 5′-cgactgggtgacaatagattaagacaagtggctaatttatagataaa-3′ were used to introduce by site-directed mutagenesis (Stratagene) a T→G at position 53 in the *IFNL3*-G ΔARE and individual mutant ARE constructs.

miRNA-target pairing site prediction

Bioinformatic analysis using RNAhybrid (version 2.2) revealed a potential miRNA binding site for the myomiR family members miR-208b and miR-499a-5p at rs4803217 in the *IFNL3*-T and *IFNL2* 3′ UTRs. Nucleotide positions 43 to 59 in the *IFNL3*-T 3′ UTR were predicted to pair with these myomiRs.

Cell transfections and reporter assays

For luciferase assays, HepG2 or Huh7 cells were plated at a density of 1×10^4 cells/well in a 96-well plate and grown overnight. Cells were transfected with 20–40 ng/well of pGL3 and 0.1–0.5 ng/well of *Renilla* reporter constructs with 0.2μl/well of X-tremeGENE 9 DNA transfection reagent (Roche). Co-transfection experiments with 20 nM of myomiR mimics (miR-208b and miR-499a-5p; Dharmacon) were conducted with 0.1–0.2 μl/well of DharmaFECT Duo transfection reagent (Dharmacon). A negative control (NC) mimic that does not bind to any target in mammalian genes (Dharmacon) was included in all experiments as necessary. After 48 h of incubation, the cells were lysed and the firefly and *Renilla* luciferase activities were measured with the Dual-Luciferase Reporter Assay System (Promega) using a multi-mode microplate reader (Synergy HT, BioTek). Luciferase activity is plotted as percent ratio of Luciferase/*Renilla*. For co-expression experiments using mCherry and eGFP reporter constructs, Huh7 cells (either HCV-infected or uninfected) were transfected using 1 μl/well in a 48-well plate of DharmaFECT Duo transfection reagent with 50 ng of total plasmid (controls and *IFNL3* 3′ UTR reporters were mixed in a 1:1 ratio) along with 40 nM of a cocktail of locked nucleic acid inhibitors (LNA) against miR-208b and miR-499a-5p (designed with Exiqon). The negative control inhibitor was an LNA mismatched against miR-208b and miR-499a-5p. For studies on the endogenous regulation of *IFNL2* and *IFNL3* mRNA by HCV-induced myomiRs, Huh7 cells were plated at a density of 3×10^5 cells/well in 2 ml of a 6-well plate and 8 h later transfected with 40 nM of inhibitors (myomiRs or NC). 16 h post-transfection, cells were washed and replated into 12-well dishes at a density of 1×10^5 cells/well and infected with HCV after 6 h.

To study the effect of miR-208b and miR-499a-5p on endogenous *IFNL2* and *IFNL3* expression, HepG2 cells were plated at a density of 3×10^5 cells/well in a 6-well plate in 2 ml and grown overnight. 20 nM of mimics were transfected with 5 μl of DharmaFECT 4

transfection reagent per well. After 24 h of incubation, cells were transfected/stimulated with 3 μg/well of Poly(I:C) (InvivoGen) using 3 μl/well of X-tremeGENE 9 transfection reagent according to the manufacturer's instructions (Roche). For experiments involving the HCV 3′ poly U/UC PAMP[33,47], 20 nM of mimics were co-transfected with 100 or 500 ng of the PAMP into HepG2 cells using 3 μl of DharmaFECT Duo transfection reagent per well.

pLV-miRNA overexpressing lines

Lentiviral vectors producing miR-208b or miR-499a-5p were transduced into HepG2 cells by lentiviral infection as previously described[48]. Briefly, self-inactivating pLV-miR-208b, pLV-miR-499a-5p or pLV-control (Biosettia) were used to generate vesicular stomatitis virus-pseudotyped lentiviral vectors. pLV constructs were transfected into HEK293FT cells using FuGENE 6 (Roche) according to the manufacturer's instruction. HepG2 cells were transduced by lentivirus. Post-transduction the cells were selected with 5 μg/ml puromycin (Sigma-Aldrich). The levels of miRNA expression were evaluated by real-time PCR probing for mature miR-208b and miR-499-5p.

RNA and miRNA expression analysis by RT-PCR

RNA was extracted using the RNeasy Kit (Qiagen) and reverse transcribed using the QuantiTect RT kit (Qiagen). RT-PCR primers/probe previously designed and tested for specificity were used to detect *IFNL2* and *IFNL3*[21]: 900 nM *IFNL2* forward (5′-gaaggttctggaggccacc-3′) and 900 nM *IFNL2* reverse (5′-ggctggtccaagacgtcca-3′); 900 nM *IFNL3* forward 5′-gaaggttctggaggccacc-3′ and 900 nM *IFNL3* reverse 5′-ggctggtccaagacatcc-3′; 250 nM probe 5′FAM-gctgacactgacccagccctgg-TAMRA-3′. Relative quantification of human *IFNB1*, *MYH6*, *MYH7*, *MYH7B* and pri-miR-499a was performed using TaqMan RT-PCR assays (Life Technologies). *HPRT* and *GAPDH* (Integrated DNA Technologies) were used as endogenous controls.

miRNA was extracted using Trizol (Invitrogen). Relative quantification of mature hsa-miR-208b and hsa-miR-499a-5p was performed using miRCURY LNA Universal RT microRNA PCR assays according to the manufacturer's instructions (Exiqon). Among the commercially available microRNA primers, we found the Exiqon LNA primers for miR-208b and miR-499a-5p to have superior efficiency. Three Exiqon LNA primers designed to detect the most common mature miR-499a-5p isomiRNAs (miRBase) were pooled for detection. The miR-208b Exiqon LNA primer was optimized by using primers with lower Tm. SNORD38B was used as an endogenous control. mRNA stability experiments were performed using 10 μg of Actinomycin D (Act D) per 1×10^6 cells/ml. For stability of the firefly luciferase mRNA, total RNA was extracted (Qiagen) and polyadenylated mRNA was purified from the preparation using a Dynabead mRNA Purification Kit (Ambion/Life Technologies). Firefly luciferase mRNA was detected using custom designed TaqMan primers (Life Technologies). No RT controls were included and showed no amplification.

Flow cytometry

Flow cytometry was performed on Huh7 cells using an LSRII (BD Biosciences). For all experiments, cells were fixed in 3% paraformaldehyde in 1× PBS for 30 min.

Co-immunoprecipitation of mRNA and miRNA from miRISC complex

mRNA:miRNA-protein complexes were immunoprecipitated (IP) as previously described[49]. Briefly, 3×10^6 HepG2 cells were plated in 10 cm^2 dishes and grown overnight. Each plate was co-transfected with 20 nM of NC mimics or a cocktail of miR-208b and miR-499a-5p as well as 2 μg HCV PAMP using 5 μl DharmaFECT Duo transfection reagent. At 16 h post-transfection the cells were lysed in polysome lysis buffer. An aliquot of the lysate was taken to obtain the input *HPRT* mRNA values for normalization. Lysates were precleared for 1 h with protein G beads (GE Healthcare 17-0618-02) followed by overnight IP with 10 μg of control IgG or anti-Ago2 antibody (Wako 015-22031) conjugated to protein G beads. IPs were washed with polysome lysis buffers and aliquots were taken for Western blot analysis of Ago2 and for RNA detection of *IFNL2*, *IFNL3*, miR-208b and miR-499a-5p.

Virus infection of Huh7 and Huh7.5 cell lines

Cell culture adapted HCV JFH1 genotype 2A strain was propagated and infectivity titrated by focus forming assay, as previously described[50]. For HCV infection experiments, cells were inoculated with virus (MOI 0.3 or MOI 10 where indicated) for 3 h and then the media was replaced. Cells were harvested with Trizol at the indicated times. HCV RNA copy number was measured by quantitative real-time PCR using the TaqMan Fast Virus 1-step kit and primers specific for the 5′UTR (Pa03453408_s1, Life Technologies). The copy number was calculated by comparison to a standard curve of *in vitro* transcribed full-length HCV RNA. Sendai virus strain Cantell was obtained from Charles River Laboratory. West Nile virus (TX strain[51]) stocks were generated by a single round of amplification on Vero-E6 (ccl-81; ATCC) cells and supernatants were collected, aliquoted, and stored at −80°C. Virus stocks were titered by a standard plaque assay on BHK21 cells as previously described[52].

Liver biospecimens

Liver tissue of chronic hepatitis C infected or control livers were obtained with the approval of the university Institutional Review Board, and the participants provided written informed consent approved by our ethics committee. Unused samples from percutaneous biopsies of patients with chronic hepatitis C with no pathological evidence of fibrosis (mild HCV; Metavir grade 1, stage 0) were analyzed (n=8). Control liver tissue was obtained from unused donor liver (n=6) with IRB approval. All liver samples were flash frozen in liquid nitrogen upon collection and stored at −80°C.

Supplementary Material

Refer to Web version on PubMed Central for supplementary material.

Acknowledgments

This project has been funded by the Department of Immunology, University of Washington (R.S.), NIH grants AI060389 and AI88778 (M.G.), NIH CA148068 (C.H.) and in part with federal funds from the Frederick National Laboratory for Cancer Research, National Institutes of Health, under contract HHSN261200800001E and the Intramural Research Program of NIH, Frederick National Laboratory for Cancer Research, Center for Cancer Research (E.B., B.A.S., and M.C.). We thank P. Fink, D. Stetson, E. Clark and C. Lim for critical reading of the manuscript and S. Badil and M. Hong for technical assistance.

REFERENCES

1. Ghany MG, et al. An update on treatment of genotype 1 chronic hepatitis C virus infection: 2011 practice guideline by the American Association for the Study of Liver Diseases. Hepatoloy. 2011; 54:1433–1444.
2. Pearlman BL. Protease inhibitors for the treatment of chronic hepatitis C genotype-1 infection: the new standard of care. The Lancet Infect. Dis. 2012; 12:717–728.
3. Suppiah V, et al. IL28B is associated with response to chronic hepatitis C interferon-alpha and ribavirin therapy. Nat. Gen. 2009; 41:1100–1104.
4. Tanaka Y, et al. Genome-wide association of IL28B with response to pegylated interferon-alpha and ribavirin therapy for chronic hepatitis C. Nat. Gen. 2009; 41:1105–1109.
5. Ge D, et al. Genetic variation in IL28B predicts hepatitis C treatment-induced viral clearance. Nature. 2009; 461:399–401. [PubMed: 19684573]
6. Rauch A, et al. Genetic variation in IL28B is associated with chronic hepatitis C and treatment failure: a genome-wide association study. Gastroenterology. 2010; 138:1338–1345. 1345 e1331 1337. [PubMed: 20060832]
7. Thomas DL, et al. Genetic variation in IL28B and spontaneous clearance of hepatitis C virus. Nature. 2009; 461:798–801. [PubMed: 19759533]
8. Kotenko SV, et al. IFN-lambdas mediate antiviral protection through a distinct class II cytokine receptor complex. Nat.Immunol. 2003; 4:69–77. [PubMed: 12483210]
9. Sheppard P, et al. IL-28, IL-29 and their class II cytokine receptor IL-28R. Nat.Immunol. 2003; 4:63–68. [PubMed: 12469119]
10. Witte K, Witte E, Sabat R, Wolk K. IL-28A, IL-28B, and IL-29: promising cytokines with type I interferon-like properties. Cytokine Growth Factor Rev. 2010; 21:237–251. [PubMed: 20655797]
11. Sommereyns C, Paul S, Staeheli P, Michiels T. IFN-lambda (IFN-lambda) is expressed in a tissue-dependent fashion and primarily acts on epithelial cells in vivo. PLoS Pathog. 2008; 4:e1000017. [PubMed: 18369468]
12. Balagopal A, Thomas DL, Thio CL. IL28B and the control of hepatitis C virus infection. Gastroenterology. 2010; 139:1865–1876. [PubMed: 20950615]
13. Friborg J, et al. Combinations of Lambda Interferon with Direct-Acting Antiviral Agents Are Highly Efficient in Suppressing Hepatitis C Virus Replication. Antimicrob. Agents Ch. 2013; 57:1312–1322.
14. Dickensheets H, Sheikh F, Park O, Gao B, Donnelly RP. Interferon-lambda (IFN-lambda) induces signal transduction and gene expression in human hepatocytes but not in lymphocytes or monocytes. J. Leukocyte Biol. 2012
15. Honda M, et al. Hepatic ISG expression is associated with genetic variation in interleukin 28B and the outcome of IFN therapy for chronic hepatitis C. Gastroenterology. 2010; 139:499–509. [PubMed: 20434452]
16. McGilvray I, et al. Hepatic cell-type specific gene expression better predicts HCV treatment outcome than IL28B genotype. Gastroenterology. 2012; 142:1122–1131. e1121. [PubMed: 22285807]
17. Naggie S, et al. Dysregulation of innate immunity in hepatitis C virus genotype 1 IL28B-unfavorable genotype patients: impaired viral kinetics and therapeutic response. Hepatology. 2012; 56:444–454. [PubMed: 22331604]
18. Langhans B, et al. Interferon-lambda serum levels in hepatitis C. J. Hepatol. 2011; 54:859–865. [PubMed: 21145813]
19. Raglow Z, Thoma-Perry C, Gilroy R, Wan YJ. IL28B genotype and the expression of ISGs in normal liver. Liver Int. 2013
20. Yoshio S, et al. Human blood dendritic cell antigen 3 (BDCA3)(+) dendritic cells are a potent producer of interferon-lambda in response to hepatitis C virus. Hepatology. 2013; 57:1705–1715. [PubMed: 23213063]

21. Urban TJ, et al. IL28B genotype is associated with differential expression of intrahepatic interferon-stimulated genes in patients with chronic hepatitis C. Hepatology. 2010; 52:1888–1896. [PubMed: 20931559]
22. di Iulio J, et al. Estimating the net contribution of interleukin-28B variation to spontaneous hepatitis C virus clearance. Hepatology. 2011; 53:1446–1454. [PubMed: 21360716]
23. de Castellarnau M, et al. Deciphering the interleukin 28B variants that better predict response to pegylated interferon-alpha and ribavirin therapy in HCV/HIV-1 coinfected patients. PloS ONE. 2012; 7:e31016. [PubMed: 22328925]
24. Pedergnana V, et al. Analysis of IL28B variants in an Egyptian population defines the 20 kilobases minimal region involved in spontaneous clearance of hepatitis C virus. PloS ONE. 2012; 7:e38578. [PubMed: 22719902]
25. Seko Y, Cole S, Kasprzak W, Shapiro BA, Ragheb JA. The role of cytokine mRNA stability in the pathogenesis of autoimmune disease. Autoimmun. Rev. 2006; 5:299–305. [PubMed: 16782553]
26. Chen JM, Ferec C, Cooper DN. A systematic analysis of disease-associated variants in the 3' regulatory regions of human protein-coding genes II: the importance of mRNA secondary structure in assessing the functionality of 3' UTR variants. Hum. Genet. 2006; 120:301–333. [PubMed: 16807757]
27. Meisner NC, et al. mRNA openers and closers: modulating AU-rich element-controlled mRNA stability by a molecular switch in mRNA secondary structure. Chembiochem : Eur. J. Chem. Biol. 2004; 5:1432–1447.
28. Manry J, et al. Evolutionary genetic dissection of human interferons. J. Exp. Med. 2011; 208:2747–2759. [PubMed: 22162829]
29. Kulkarni S, et al. Differential microRNA regulation of HLA-C expression and its association with HIV control. Nature. 2011; 472:495–498. [PubMed: 21499264]
30. Guo H, Ingolia NT, Weissman JS, Bartel DP. Mammalian microRNAs predominantly act to decrease target mRNA levels. Nature. 2010; 466:835–840. [PubMed: 20703300]
31. O'Neill LA, Sheedy FJ, McCoy CE. MicroRNAs: the fine-tuners of Toll-like receptor signalling. Nat. Rev. Immunol. 2011; 11:163–175. [PubMed: 21331081]
32. van Rooij E, et al. A family of microRNAs encoded by myosin genes governs myosin expression and muscle performance. Dev. Cell. 2009; 17:662–673. [PubMed: 19922871]
33. Schnell G, Loo YM, Marcotrigiano J, Gale M Jr. Uridine composition of the poly-U/UC tract of HCV RNA defines non-self recognition by RIG-I. PLoS Pathog. 2012; 8:e1002839. [PubMed: 22912574]
34. Foy E, et al. Control of antiviral defenses through hepatitis C virus disruption of retinoic acid-inducible gene-I signaling. Proc. Natl. Acad. Sci. USA. 2005; 102:2986–2991. [PubMed: 15710892]
35. Li X-D, Sun L, Seth RB, Pineda G, Chen ZJ. Hepatitis C virus protease NS3/4A cleaves mitochondrial antiviral signaling protein off the mitochondria to evade innate immunity. Proc. Natl. Acad. Sci. USA. 2005; 102:17717–17722. [PubMed: 16301520]
36. Sumpter R Jr, et al. Regulating intracellular antiviral defense and permissiveness to hepatitis C virus RNA replication through a cellular RNA helicase, RIG-I. J.Virol. 2005; 79:2689–2699. [PubMed: 15708988]
37. Saito T, et al. Regulation of innate antiviral defenses through a shared repressor domain in RIG-I and LGP2. Proc. Natl. Acad. Sci. USA. 2007; 104:582–587. [PubMed: 17190814]
38. Chugh P, Dittmer DP. Potential pitfalls in microRNA profiling. Wiley Interdiscip. Rev. RNA. 2012; 3:601–616. [PubMed: 22566380]
39. Leshkowitz D, Horn-Saban S, Parmet Y, Feldmesser E. Differences in microRNA detection levels are technology and sequence dependent. RNA. 2013; 19:527–538. [PubMed: 23431331]
40. Janssen HLA, et al. Treatment of HCV Infection by Targeting MicroRNA. N. Engl. J. Med. 2013; 368:1685–1694. [PubMed: 23534542]
41. Matsumori A. Hepatitis C virus infection and cardiomyopathies. Circ. Res. 2005; 96:144–147. [PubMed: 15692092]

42. Lauer B, Schannwell M, Kuhl U, Strauer BE, Schultheiss HP. Antimyosin autoantibodies are associated with deterioration of systolic and diastolic left ventricular function in patients with chronic myocarditis. J. Am. Coll. Cardiol. 2000; 35:11–18. [PubMed: 10636253]

43. Caforio AL, et al. Clinical implications of anti-heart autoantibodies in myocarditis and dilated cardiomyopathy. Autoimmunity. 2008; 41:35–45. [PubMed: 18176863]

44. Dellgren C, Gad HH, Hamming OJ, Melchjorsen J, Hartmann R. Human interferon-lambda3 is a potent member of the type III interferon family. Genes Immun. 2009; 10:125–131. [PubMed: 18987645]

45. Prokunina-Olsson L, et al. A variant upstream of IFNL3 (IL28B) creating a new interferon gene IFNL4 is associated with impaired clearance of hepatitis C virus. Nat. Gen. 2013

ONLINE METHODS REFERENCES

46. Lorenz R, et al. ViennaRNA Package 2.0. Algorithm. Mol. Biol. 2011; 6:26.

47. Saito T, Owen DM, Jiang F, Marcotrigiano J, Gale M Jr. Innate immunity induced by composition-dependent RIG-I recognition of hepatitis C virus RNA. Nature. 2008; 454:523–527. [PubMed: 18548002]

48. Savan, R.; Chan, T.; Young, HA. Natural Killer Cell Protoc. Springer; 2010. p. 209-221.

49. Peritz T, et al. Immunoprecipitation of mRNA-protein complexes. Nat. Protoc. 2006; 1:577–580. [PubMed: 17406284]

50. Kato T, et al. Cell culture and infection system for hepatitis C virus. Nat. Protoc. 2006; 1:2334–2339. [PubMed: 17406476]

51. Keller BC, et al. Resistance to alpha/beta interferon is a determinant of West Nile virus replication fitness and virulence. J. Virol. 2006; 80:9424–9434. [PubMed: 16973548]

52. Diamond MS, Shrestha B, Marri A, Mahan D, Engle M. B cells and antibody play critical roles in the immediate defense of disseminated infection by West Nile encephalitis virus. J. Virol. 2003; 77:2578–2586. [PubMed: 12551996]

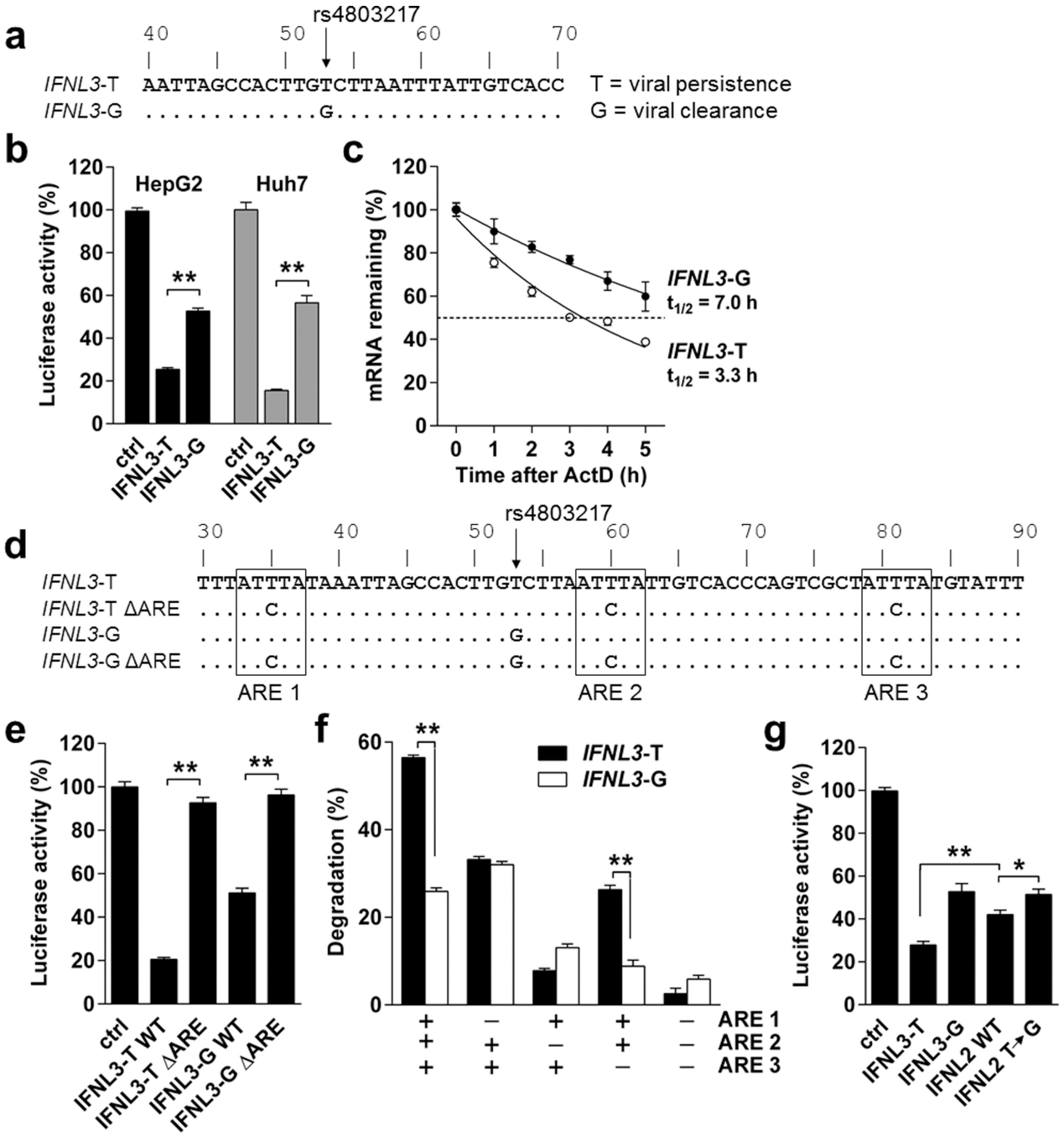

Figure 1.

IFNL3 rs4803217 3′ UTR variants are differentially regulated and are subject to ARE-mediated decay. (**a**) Alignment of *IFNL3-T* and *IFNL3-G* 3′ UTR sequences (nt 40 to 70). SNP rs4803217 at nt position 53 is indicated with an arrow. (**b**) HepG2 or Huh7 cells were transfected with the indicated constructs. Data are plotted as the percent Luciferase/*Renilla* ratio compared to the mean activity of the control construct. (**c**) *IFNL3*-T or *IFNL3*-G luciferase constructs were transfected into HepG2 cells and treated with Act D to arrest new transcription. Stability was determined as percent luciferase mRNA remaining over time,

compared to 0 h. Half-life ($t_{1/2}$) of luciferase mRNA bearing the *IFNL3*-G 3′ UTR was 7.0 h (R^2 = 0.82) compared to 3.3 h for the luciferase mRNA bearing the *IFNL3*-T 3′ UTR (R^2 = 0.95). Data represent mean ± s.e.m. from one of three comparable experiments. (**d**) Alignment of *IFNL3* 3′ UTR sequences (nt 30 to 90) showing AU-rich elements (ARE 1–3, boxed) and mutations introduced to disrupt the motifs (ΔARE, ATTTA→ATCTA). (**e–g**) HepG2 cells were transfected with the indicated constructs. Data are plotted as the percent Luciferase/*Renilla* ratio compared to the activity of the control construct. (**f**) Data are plotted as the percent degradation compared to the luciferase activity of the control construct (set at 0%). (**b, e-g**) Data represent six replicates in each experimental group plotted as mean ± s.e.m. from one representative of three or more experiments. Unpaired t tests (**e, g**) or two-way analysis of variance (**f**) were used for statistical comparisons and two-tailed *P* values are given. *P<0.05, **P≤0.0005.

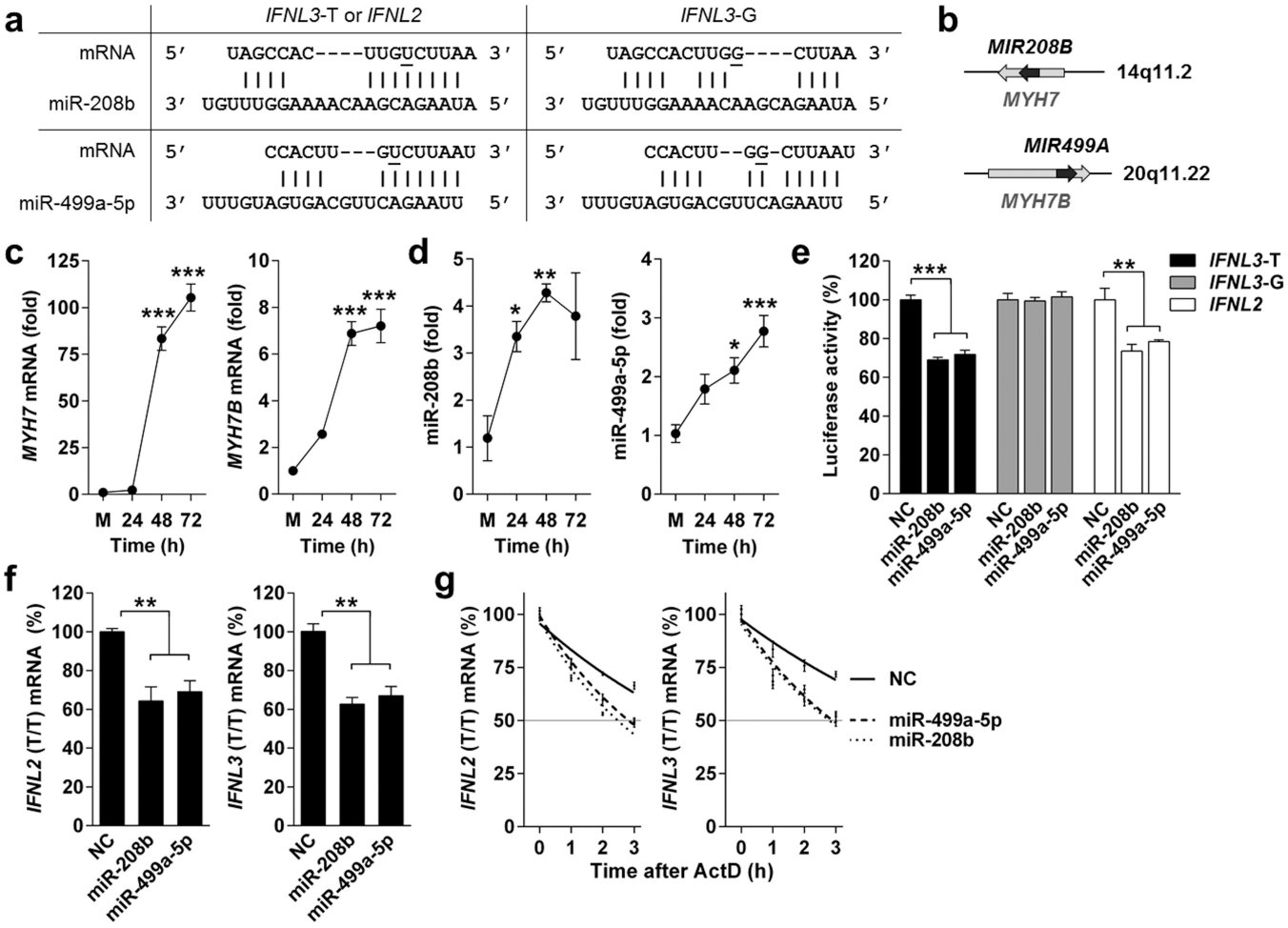

Figure 2.

Variation in the *IFNL3* 3′ UTR mediates post-transcriptional repression by HCV-induced myomiRs, miR-208b and miR-499a-5p. (**a**) RNAhybrid analysis was used to show the miRNA:target interaction for hsa-miR-208b and hsa-miR-499a-5p which bind at nucleotide positions 43 to 58 of the *IFNL3*-T and *IFNL2* 3′ UTRs. The rs4803217 T→G SNP (underlined) is located at nucleotide position 53 in the mRNA. (**b**) Schematic showing the chromosomal location of the human *MYH7* and *MYH7B* genes (grey arrows) and the intronic miRNAs, *MIR208B* and *MIR499A* (black arrows), that they encode. (**c, d**) Huh7 cells were infected with HCV for 24, 48 and 72 h and expression of *MYH7*, *MYH7B*, miR-208b and miR-499a-5p was assessed. Reference sample for relative quantification was mock infected cells taken at 48 h. Data represent mean ± s.e.m. of four individual experiments pooled. One-way analysis of variance was used for statistical comparisons across the time points compared to the mock (M) infection. (**e**) HepG2 cells were co-transfected with the indicated *IFNL* 3′ UTR luciferase reporter constructs along with the indicated mimics (NC, negative control). Data are plotted as the percent Luciferase/*Renilla* ratio compared to the mean activity of each construct co-transfected with NC mimics. Data represent six replicates in each experimental group plotted as mean ± s.e.m. from one representative of three experiments. Unpaired t tests were used for statistical comparisons and two-tailed *P* values

are given. (**f**) HepG2 cells were transfected with the indicated mimics and then stimulated with Poly(I:C). *IFNL2* and *IFNL3* mRNA levels were assessed and are plotted as percent expression compared to cells transfected with NC mimics. Data represent mean ± s.e.m. and are pooled from three individual experiments. Unpaired t tests were used for statistical comparisons and two-tailed *P* values are given. (**g**) HepG2 cells were co-transfected with HCV PAMP and the indicated mimics. Act D was added 16 h post-transfection and the percent of *IFNL2* (T/T) and *IFNL3* (T/T) mRNA remaining over time was assessed. All curve fits for *IFNL2* and *IFNL3* mRNA degradation over time had $R^2 \geq 0.85$. Comparison of Fits showed differences in *IFNL2* and *IFNL3* mRNA stability were significantly different ($P<0.0001$ and $P=0.0005$, respectively). The mRNA half-lives (50% mRNA remaining, $t_{1/2}$) for the *IFNL2* mRNA were NC $t_{1/2}$ = 4.5 h, miR-208b $t_{1/2}$ = 2.4 h, miR-499a-5p $t_{1/2}$ = 2.7 h and for *IFNL3* mRNA were NC $t_{1/2}$ = 5.4 h, miR-208b $t_{1/2}$ = 3.1 h, miR-499a-5 $t_{1/2}$ = 3.2 h. Data represent mean ± s.e.m. and one of two comparable experiments performed is shown. **P*<0.05, ***P*<0.01, ****P*<0.001.

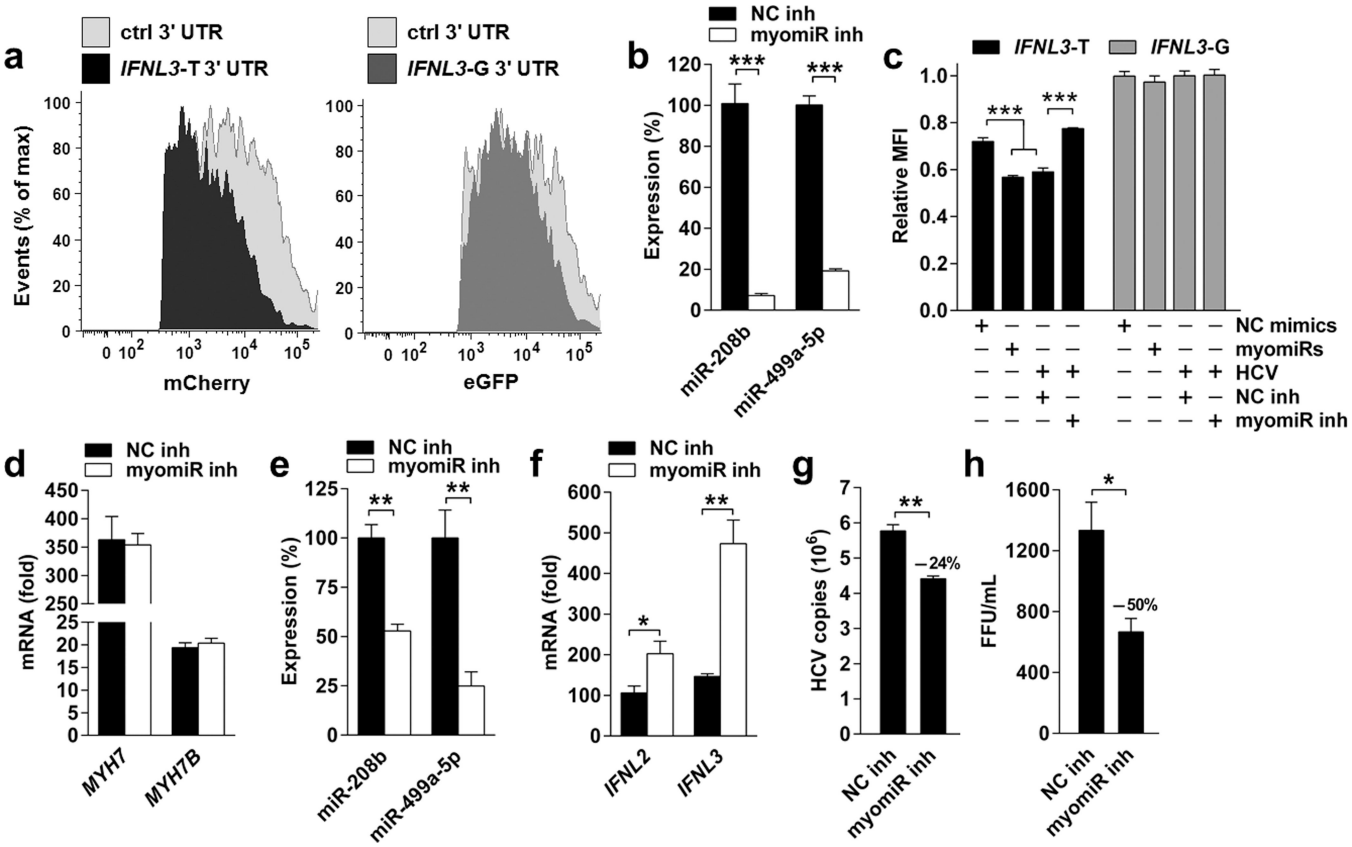

Figure 3.

Inhibition of HCV-induced myomiRs increases *IFNL2* and *IFNL3* expression as well as the antiviral response. (**a**) Mixes of mCherry and eGFP control 3′ UTR reporters or mCherry-*IFNL3*-T and eGFP-*IFNL3*-G 3′ UTR reporters were co-transfected into Huh7 cells and fluorescence was analyzed by flow cytometry after 48 h. Shown are histogram plots of *IFNL3*-T and *IFNL3*-G expression versus their controls. (**b**) To test the efficiency of LNA inhibitors designed against miR-208b and miR-499a-5p, HepG2 cells stably expressing miR-208b or miR-499a-5p were transfected with the inhibitors and miRNA expression was measured by RT-PCR. Efficiency of inhibition was >75% with 40 nM of inhibitors 48 h post-transfection. (**c**) HCV-infected Huh7 cells were co-transfected with mixes of the reporter constructs (either controls or *IFNL3* 3′ UTRs) shown in (**a**) and after 48 h the mean fluorescent intensities (MFI) were determined. Data is normalized to MFIs of the 3′ UTR control reporters and then plotted as relative expression to *IFNL3*-G treated with NC. (**d–h**) The myomiR inhibitors were transfected into Huh7 cells 24 h prior to infection with HCV. Expression analysis of *MYH7* and *MYH7B* (**d**), miR-208b and miR-499a-5p (**e**), *IFNL2* and *IFNL3* (**f**), and quantification of HCV viral copy number and titer (**g** and **h**) was carried out 72 h post-infection. Reference sample for relative quantification was mock infected cells. (**b–h**) Data represent mean ± s.e.m. and one of three comparable experiments performed is shown. Unpaired t tests were used for statistical comparisons and two-tailed *P* values are given. **P*<0.05, ***P*<0.01, ****P*<0.001.

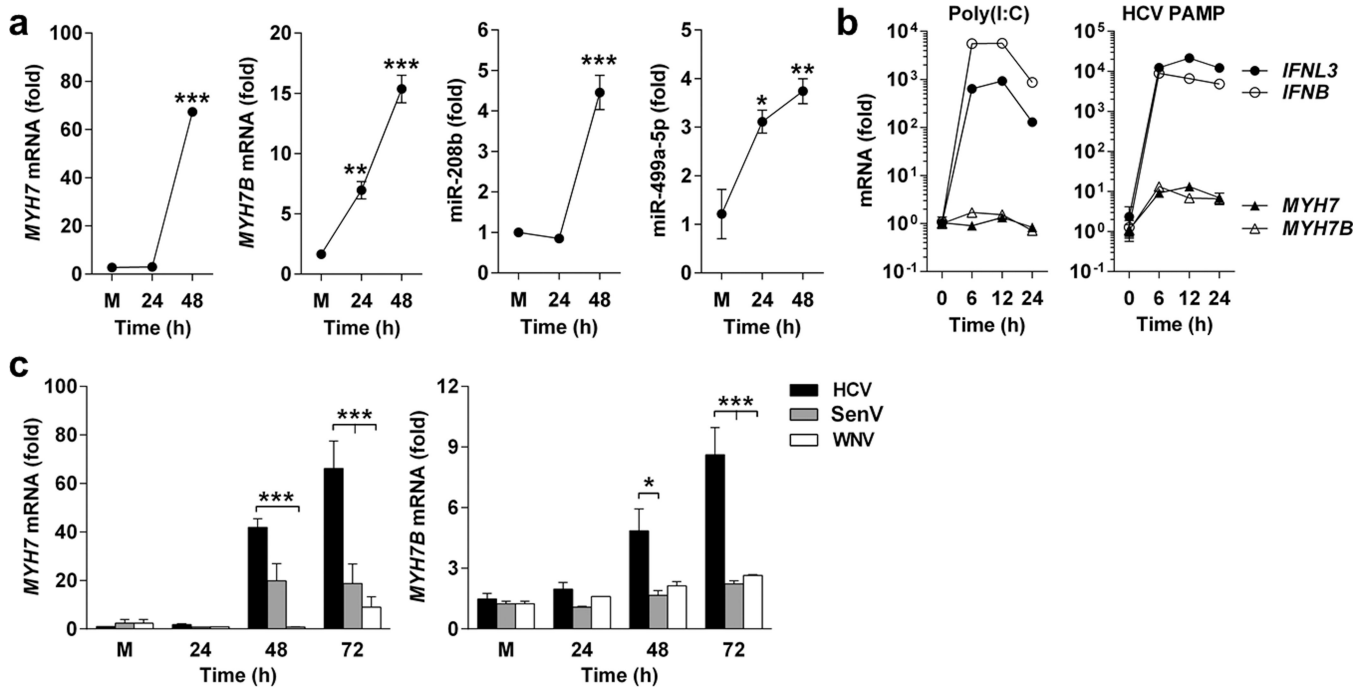

Figure 4.

Induction of *MYH7* and *MYH7B* is HCV infection-specific. (**a**) Huh7.5 cells were infected with HCV for 24 and 48 h and expression of *MYH7*, *MYH7B*, miR-208b and miR-499a-5p was assessed. Reference sample for relative quantification was mock (M) infected cells taken at 48 h. Data represent mean ± s.e.m. and one of three comparable experiments performed is shown. One-way analysis of variance was used for statistical comparisons across the time points compared to the mock infection. (**b**) HepG2 cells were stimulated with Poly(I:C) or HCV PAMP for the indicated times. Expression of *IFNL3*, *IFNB*, *MYH7* and *MYH7B* was assessed compared to unstimulated cells. (**c**) Huh7 cells were infected with HCV, Sendai virus (SenV) or West Nile virus (WNV) for 24, 48 and 72 h. Expression of *MYH7* and *MYH7B* was assessed across the infections. Data represent mean ± s.e.m. and one of two comparable experiments performed is shown. Two-way analysis of variance was used for statistical comparisons. **P*<0.05, ***P*<0.01, ****P*<0.001.

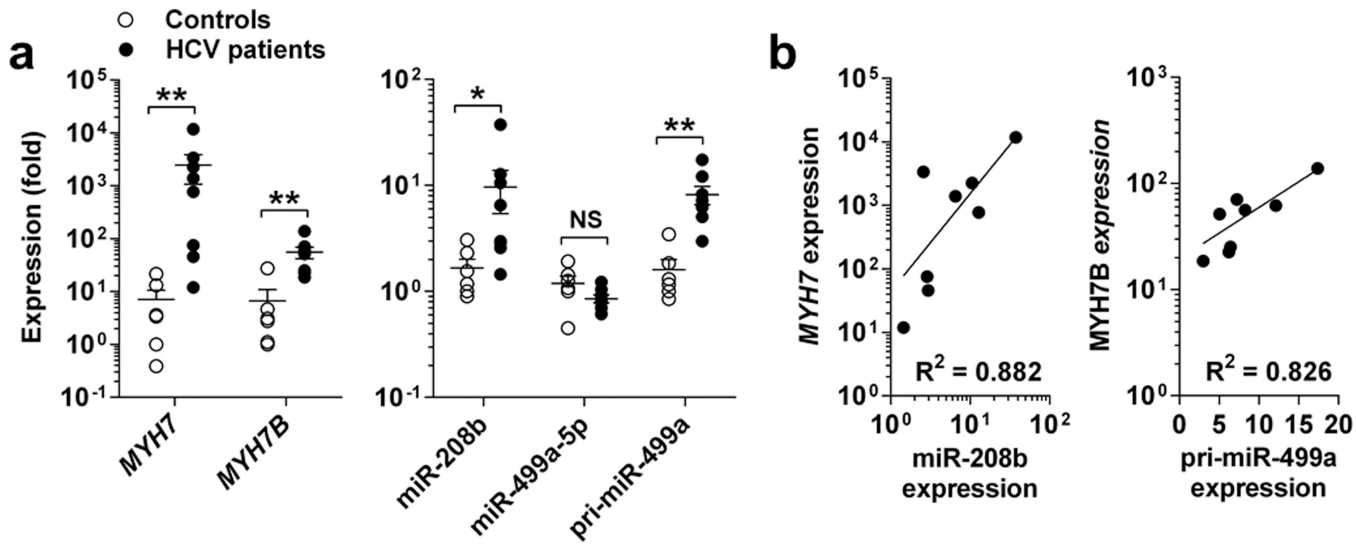

Figure 5.

Expression of myosin and myomiRs in chronic hepatitis C patients. (**a**) RNA isolated from the livers of chronic hepatitis C patients (n=8) or controls (n=6) was tested for *MYH7*, *MYH7B*, miR-208b, miR-499a-5p and pri-miR-499a-5p expression. Non-parametric Mann Whitney tests were used for statistical comparisons and two-tailed *P* values are indicated. NS, not significant, **P*=0.02, ***P*<0.005. (**b**) Correlation between *MYH7* vs. miR-208b expression (Pearson's r, *P*=0.0014) and *MYH7B* vs. pri-miR-499a-5p expression (Pearson's r, *P*=0.0033) in hepatitis C patients. R^2 values from nonlinear regressions are indicated.